MALAYSIAN JOURNAL OF SCIENCE
MJS
ISSN 1394-3065

Regular Issue

Malaysian Journal of Science 43 (3): 13-21 (September 2024) https://mjs.um.edu.my

HYDROTHERMAL SYNTHESIS OF NITROGEN-DOPED CQDS OF RUBUS NIVEUS LEAVES FOR FLUORESCENT pH SENSING AND PHOTOCATALYTIC APPLICATIONS

P. Negi[1a], B.S. Rawat[2b]*, N. C. Joshi[3c], W. Ahmad[4d], N. Kumar[5b], S. Upadhyay[6e], K. P. S. Parmar[7f], R. Saxena[8g], R. Dhyani[9h], P. S. Khati[10i], A.S. Rana[11j]

Abstract: The development of a fluorescent pH sensor and the treatment of wastewater with nanoparticles are both critical topics. Variations in pH impact the morphology and subsequent properties of nanoparticles, affecting their utilization in various fields, while using nanoparticles offers an improved approach for treating industrial waste. The present study examines the effects of these variables on biologically produced nitrogen-doped carbon quantum dots (NCQDs). The synthesis was achieved through a hydrothermal process using *Rubus niveus* leaf extract as a precursor. UV-Vis spectroscopy analysis revealed absorption spectra over a wide range from 200 nm to 800 nm, with prominent peaks at 236 nm and 392 nm. Additionally, the direct energy band gap of the NCQDs was found to be 3.65 eV. SEM imaging displayed flower-shaped particles, and FT-IR analysis indicated the presence of amide, CHO, N-H, and C-N functional groups. The XRD pattern revealed that the surface morphology of NCQDs is amorphous in nature. A significant response in fluorescence intensity with varying pH values was observed, confirming the potential of NCQDs as pH sensors. The reaction kinetics of Rhodamine-B (Rh-B) dye was analyzed to assess the potential of NCQDs for dye degradation, revealing pseudo-first-order kinetics with a correlation coefficient of 0.80.

Keywords: *hydrothermal process, pH sensor, carbon quantum dots, energy band gap, dye degradation.*

1. Introduction

Carbon quantum dots (CQDs) are emerging as a promising alternative to inorganic semiconductor materials due to their potential applications in various fields (Wang et al., 2016; Das et al., 2015; Bourlinos et al., 2013). Research highlights that low-toxicity, biocompatible, and chemically stable CQD materials are useful in drug delivery (Jallel et al., 2018), optoelectronics (Hoan et al., 2019), water treatment (Shamsipur et al., 2014), bioimaging, biomolecules (Ge et al., 2022; Basavaiah et al., 2018), and metal ion sensors (Barati et al., 2016).

The hydrothermal carbonization method is recognized as a green synthetic approach for creating CQDs. Significant efforts have been made to develop CQD fluorescent probes for metal ion detection and other applications (Du et al., 2013; Wang et al., 2011; Lin et al., 2012; Liu et al., 2012; Salinas-Castillo et al., 2013; Mosconi et al., 2015; Pires et al., 2015).

Doped CQDs offer tunable fluorescence and excellent surface passivation. The incorporation of heteroatoms, such as nitrogen, phosphorus, and sulphur, enhances the optical properties of these particles (Carolan et al., 2017). Nitrogen-doped CQDs, in particular, interact with carbon atoms by trapping radiating electron-hole pairs, forming new optical centres, and exhibiting exceptional performance in optoelectronic, electro catalytic and luminescent applications. Carbon-bonded nitrogen introduces disorder into the hexagonal carbon rings (Li et al., 2012; Krysmann et al., 2012). The advantages of CQDs over organic fluorescent dyes include their biocompatibility, low synthesis cost, electron transmission capability, water solubility, and ease of manufacture (Qu et al., 2010; Xiao et al., 2018; Zhang et al., 2016).

pH imbalances can cause various disorders by affecting the activity of several organelles, making precise measurement of intracellular pH crucial. Various materials, such as quantum dot-encoded red fluorescent protein sensors (Tantama et al., 2011), Ag@SiO2 core-shell nanoparticles (Bai et al., 2013),

Authors information:
[a]Department of Chemistry, GRD Institute of Management & Technology, Dehradun, UK, INDIA.
[b]Department of Physics, School of Applied and Life Sciences (SALS), Uttaranchal University, Dehradun-248007, UK, INDIA.
[c]Division of Research and Innovation, Uttaranchal University, Dehradun-248007, UK, INDIA.
[d]Department of Chemistry, Graphic Era University, Dehradun, UK, INDIA.
[e]Department of Allied Health Sciences, School of Health Sciences and Technology, University of Petroleum and Energy Studies, UPES, Dehradun-248007, UK, INDIA.
[f]Department of Physics, University of Petroleum and Energy Studies, UPES, Dehradun-248007, UK, INDIA.
[g]Department of Physics, Shri Guru Ram Rai University, Dehradun-248007, UK, INDIA.
[h]Department of Applied Science, Women Institute of Technology, Dehradun, 248007, INDIA.
[i]Department of Chemistry, S.D.M. PG. College Doiwala, Dehradun-248007, UK, INDIA.
[j]Department of Physics, Shri Guru Ram Rai (P.G.) College, Dehradun-248007, UK, INDIA.
*Corresponding Author: park_bhupendra@hotmail.com

Received: July 25, 2023
Accepted: September 19, 2023
Published: September 30, 2024

DOI:https//doi.org/10.22452/mjs.vol43no3.2
Malaysian Journal of Science 43(3): 9-21 (September 2024)

semiconducting polymer dots (Chan et al., 2011), and fluorescent quantum FRET probe dots (Dennis et al., 2012), have been developed for pH monitoring. However, these materials have limitations including bulkiness, severe toxicity, and biocompatibility issues. In contrast, CQDs have emerged as excellent candidates for pH testing due to several advantages (Han et al., 2010; Jin et al., 2010; Nie et al., 2014).

Moreover, prior studies have demonstrated that the presence of H^+ or OH^- ions affects the morphology of biosynthesized metal oxide nanoparticles (Zyoud et al., 2019). Changes in pH significantly impact the hydrolysis and condensation processes during the formation of the precursor solution (Arya et al., 2021). These pH fluctuations similarly influence the morphology and characteristics of biosynthesized nanoparticles, including their optical properties (Khairol et al., 2018). Recently, various plant parts have been shown to act as reducing and capping agents to create eco-friendly, non-toxic nanoparticles for diverse applications (Sathish kumar et al., 2012; Su et al., 2012; Su et al., 2005).

Rubus niveus, locally known as Kala Hisar or Mysore raspberries, is a large, spiny shrub that commonly grows along highways, in woodlands, and in mountainous regions between 1000 and 2500 m. It is noted for its antibacterial, anticancer, wound-healing, and anti-inflammatory properties. The phytochemicals responsible for these unique qualities include saponins, tannins, flavonoids, phenols, and sugars (Blassan et al., 2014; Mullen et al., 2002).

The current study focuses on the synthesis of nitrogen-doped carbon quantum dots (NCQDs) from *Rubus niveus* leaves and examines their characteristic properties, including their capacity for photocatalytic degradation and fluorescent pH sensing.

2. Experimental Methods

Fresh *Rubus niveus* leaves were collected from a location near the campus of Uttaranchal University. We employed ethylenediamine and rhodamine-B without further purification. Double-distilled to conduct the experiments

3. Synthesis of NCQDs

The synthesis of nitrogen-doped carbon quantum dots (NCQDs) was performed using a single-step hydrothermal method (Fig. 1). Initially, the leaves were collected, washed with tap water, followed by deionized (DI) water to remove dust, and then dried in an incubator at ambient conditions. Subsequently, 5 g of the dried leaves were combined with approximately 60 ml of water and heated to 200 °C for 2 hours in a Teflon-lined autoclave. After this, 1.5 ml of ethylenediamine was added to 15 ml of the resulting carbon quantum dot (CQD) solution, which was then subjected to further heating at 200 °C for an additional 3 hours. Centrifugation was performed for about 45 minutes to remove large particles from the solution, followed by filtration using micro-level filter paper. The final solid product was obtained by drying at 75 °C.

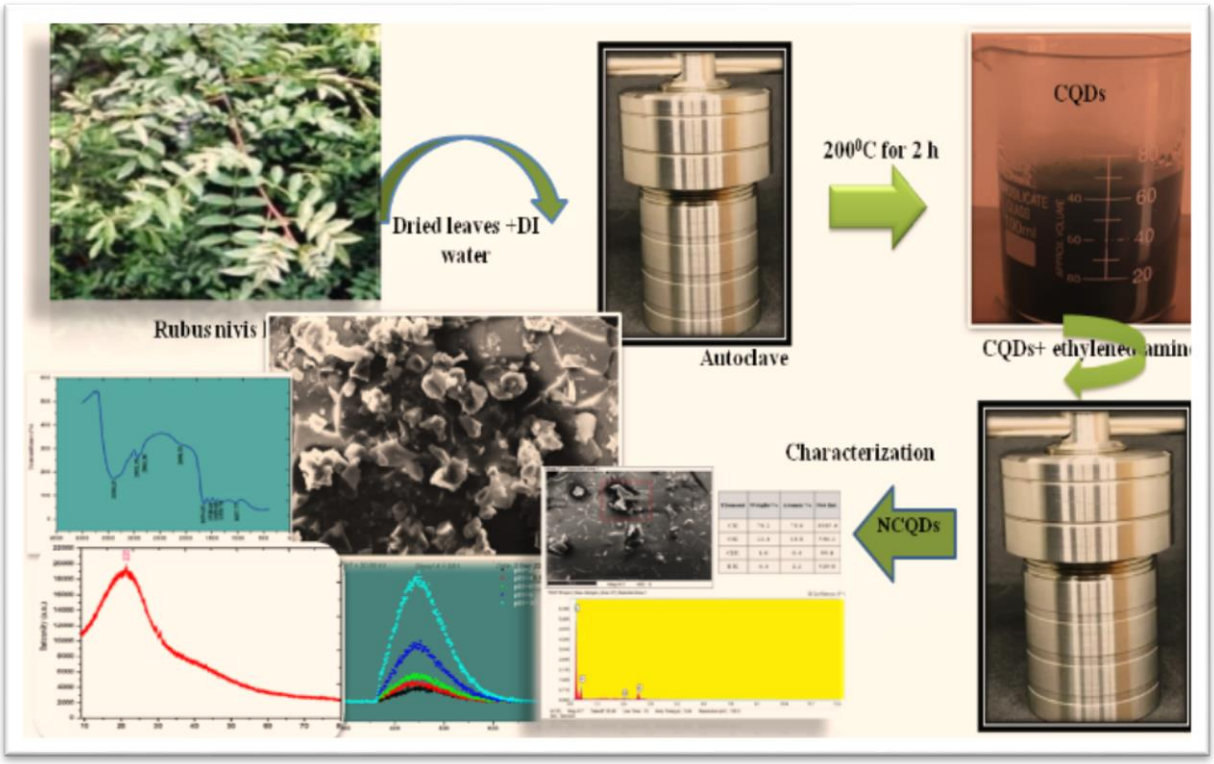

Figure1. Schematic of the synthesis of NCQDs

DOI:https//doi.org/10.22452/mjs.vol43no3.2
Malaysian Journal of Science 43(3): 9-21 (September 2024)

4. Characterizations

UV-Vis spectral analysis, Scanning Electron Microscopy (SEM), Fourier Transform Infrared Spectroscopy (FTIR), Energy Dispersive X-ray Spectroscopy (EDX),and the X-ray powder diffraction (XRD) method were employed to describe the powder morphology of NCQDs.

Optical Properties Analysis

Analyses of absorption peaks, spectral ranges, and energy band gaps were conducted at room temperature (Fig. 2). The absorption bands were observed at 236 nm and 392 nm, with the spectral range spanning from 200 nm to 800 nm. To estimate the indirect optical energy band gap, the absorption spectrum was analyzed with reference to the absorption edge using the Tauc equation (Tauc et al., 1966), a methodology well-documented in the literature (Muhammad et al., 2011; Yakuphanoglu et al., 2005). Theenergy band gap value estimation was performed by plotting $(\alpha hv)^2$ versus photon energy $hv$and found to be 3.65eV.

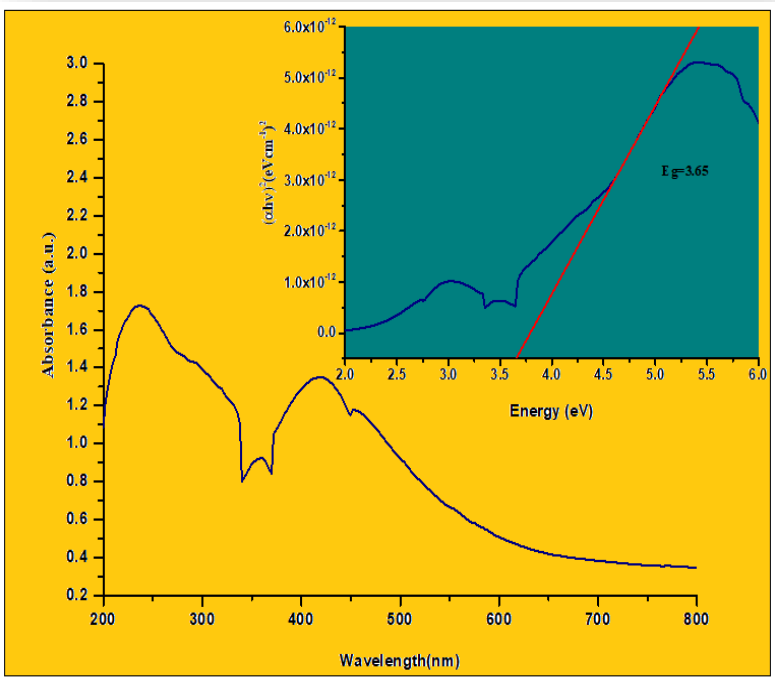

Figure 2. Plot of absorbance versus wavelength and $(\alpha hv)^2$ versus hv

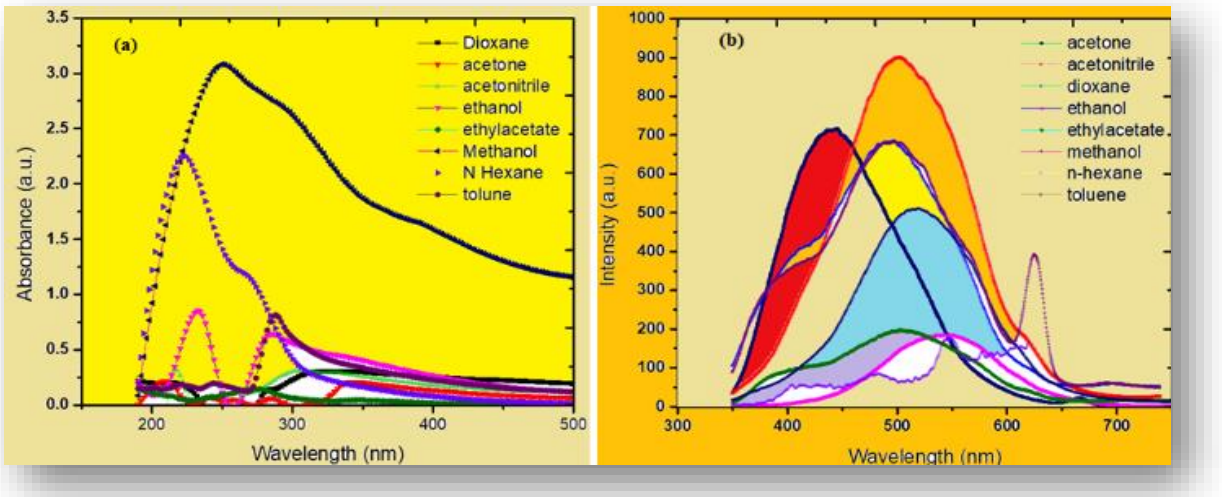

Figure 3. Plot of (a) absorbance and (b) emission versus wavelength in different solvents

DOI:https//doi.org/10.22452/mjs.vol43no3.2
Malaysian Journal of Science 43(3): 9-21 (September 2024)

The photophysical properties of NCQDs were investigated and are illustrated in Figure 3. The plots of (a) absorbance versus wavelength and (b) emission versus wavelength demonstrate the shift in peaks due to the use of different solvents, highlighting the Solvatochromic effect of the synthesized particles (Khazan et al., 2017; Dash et al., 1999). For solvents such as toluene, ethanol, dioxane, and methanol, the peaks shift towards longer wavelengths, indicating a bathochromic shift. Conversely, a hypsochromic shift is observed with ethyl acetate and acetone, with N-hexane used as the reference solvent.

The solvent-dependent shifts are attributed to the solvents' polarity and hydrogen bonding, which influence the fluorescent molecules' electronic transitions and energy levels. These findings suggest potential advantages for a broad range of industrial and technological applications.

SEM and EDX Analysis

The surface characteristics and morphological properties of NCQDs were examined using scanning electron microscopy (SEM). The SEM images of the NCQDs synthesized *from Rubus niveus* revealed flower-shaped particles with some degree of agglomeration (Fig. 4a). The observed agglomeration may be attributed to the sample preparation process.

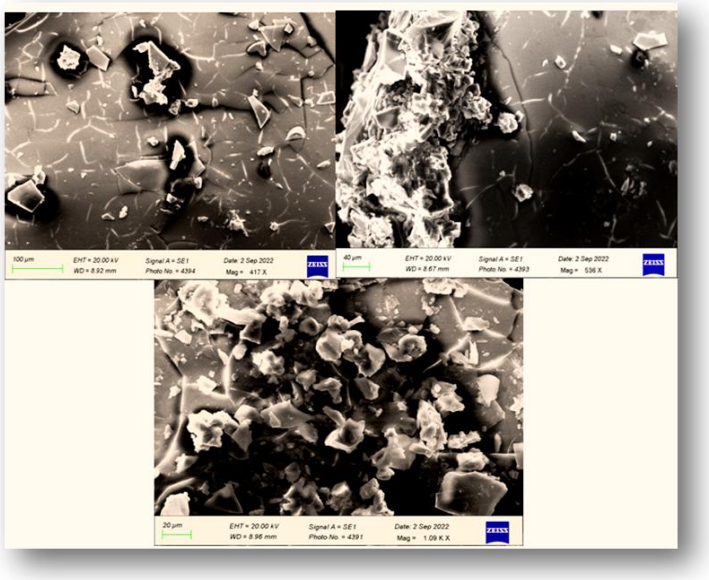

Figure 4(a). SEM morphology of NCQDs

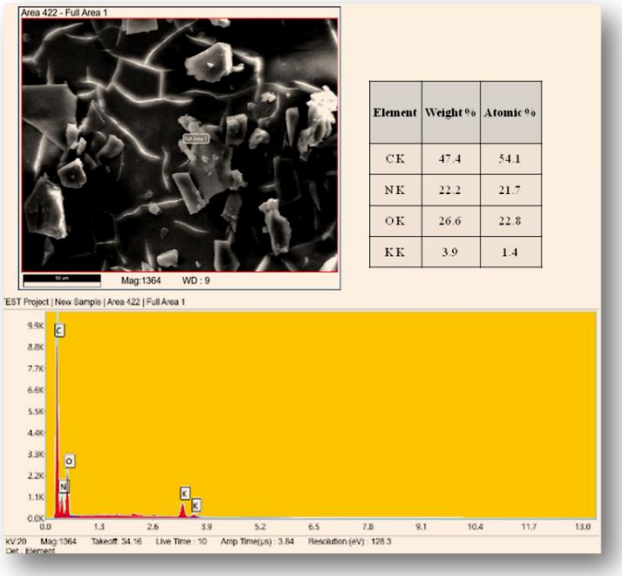

Element	Weight %	Atomic %
CK	47.4	54.1
NK	22.2	21.7
OK	26.6	22.8
KK	3.9	1.4

Figure 4 (b). EDX spectrum of NCQDs

DOI:https//doi.org/10.22452/mjs.vol43no3.2
Malaysian Journal of Science 43(3): 9-21 (September 2024)

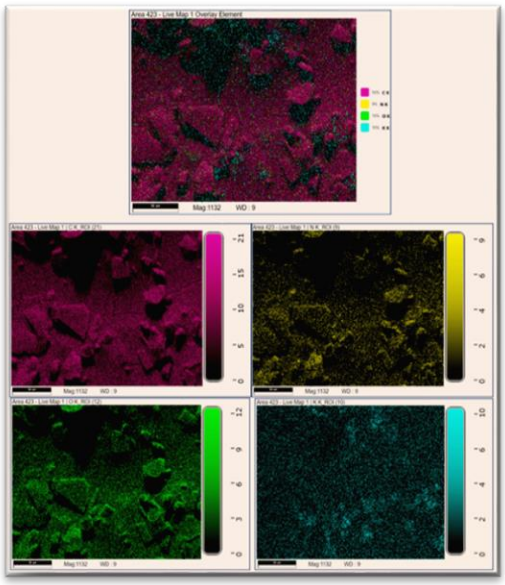

Figure.4 (b). Mapping of elements present in NCQDs

The EDX spectrum for analyzing the chemical composition of NCQDs is presented inFigure4b. The graph displays the weight and atomic percentages of the four main elements: C, N, O, and K. The presence of both carbon and nitrogen indicates successful incorporation of nitrogen into the CQDs. The detection of potassium is attributed to an incomplete washing process, which could be improved by washing with double distilled water and ethanol before drying the material. The figure shows that carbon constitutes the largest weight percentage. The presence of these elements without significant impurities confirms the purity of the synthesized NCQDs (Selva Raja et al., 2015). Elemental mapping reveals a uniform distribution of these materials throughout the synthesized NCQDs, as shown in Figure 4b.

Functional Groups Analysis

The presence of functional groups on the surface of NCQDs, which act as reducing agents during their synthesis, was investigated using FTIR analysis. A prominent peak in the FTIR spectrum (Fig. 5) at 3390 cm^{-1} corresponds to the N-H stretching vibration of secondary amines, indicating the presence of amino functional groups (Chang et al., 2022). The bands at 2932 cm^{-1} are attributed to the Fermi resonance-induced C-H stretching of aldehydes.

The C=O stretching of the amide group resultsinabandat1650cm^{-1}, while the N-H bending vibration of the amide is reflected in a troughat1548 cm^{-1}. The C-N stretching vibration of the amine is responsible for the peaks at 1350 and 1037 cm^{-1}, confirming the successful incorporation of nitrogen into the carbon dots. Furthermore, the FTIR data also verifies that the CQDs are doped with nitrogen. The presence of these functional groups, which also act as stabilizers, underscores their role in the formation of NCQDs, as observed in the plant extract.

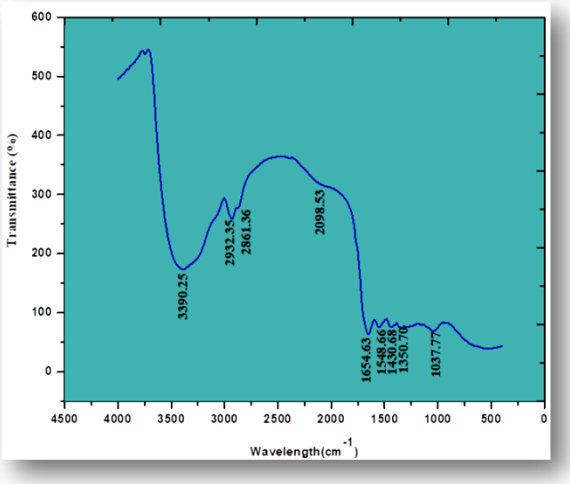

Figure 5. FT-IR spectrum for synthesized NCQDs

DOI:https//doi.org/10.22452/mjs.vol43no3.2
Malaysian Journal of Science 43(3): 9-21 (September 2024)

Crystallographic Structure Analysis

Figure (6) depicts the NCQDs' acquired XRD pattern. Comparison of the XRD pattern to the typical JCPDS card no. 00-039-1405 reveals a large and powerful diffraction peak at 2θ=21.367 with a hkl value of 220. This shows that synthesized NCQDs are amorphous.

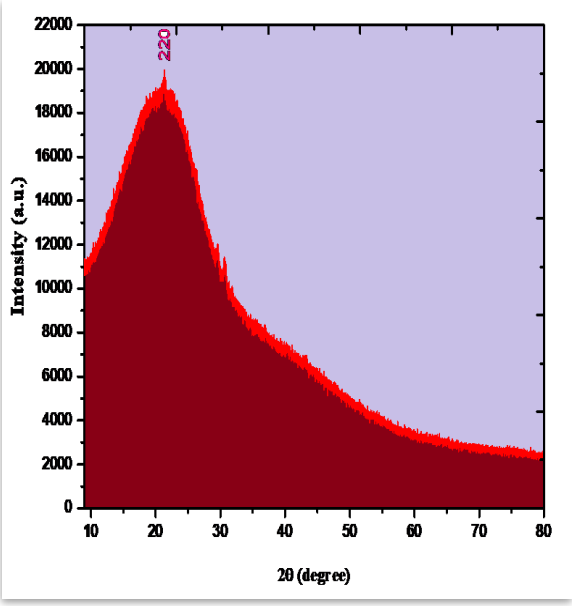

Figure 6.XRD diffractogarm for synthesized NCQDs

Analysis of p Effect on Fluorescence Emission

Figure 7a shows the produced samples, while Figure 7b illustrates the measured fluorescence intensity of solutions at various pH values. The significant shift in fluorescence intensity with wavelength, observed as the pH value changes from 2 to 10, can be explained by the numerical excitation wavelength value of the sample at 260 nm. The plot of fluorescence intensity versus pH (Figure 7c), which yields a linear correlation coefficient of 0.771, further supports this association. This demonstrates that the proposed NCQDs are promising candidates for pH measurement applications.

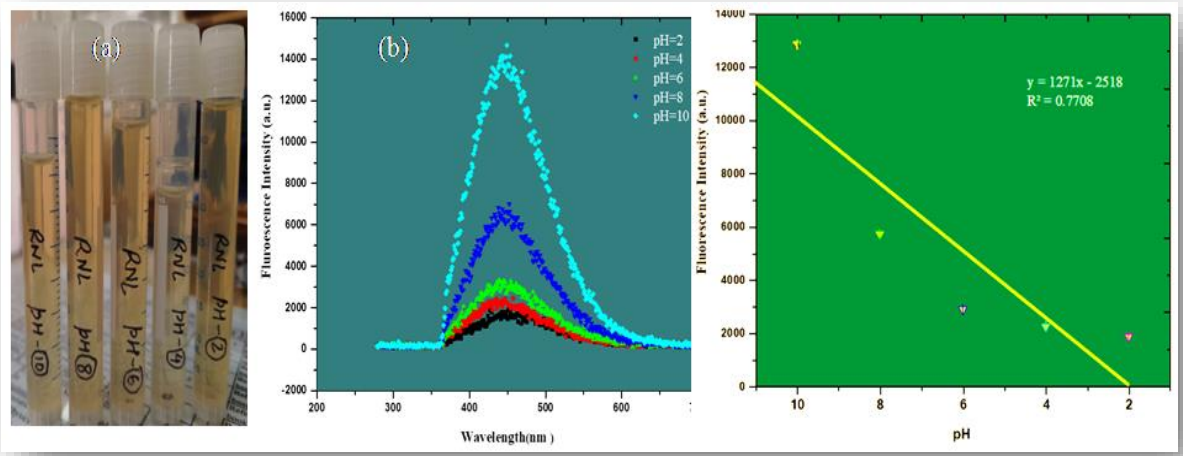

Figure 7.(a) Prepared pH samples**(b)**Intensity of fluorescence versus wavelength **(c)**Intensity versus pH values

Photocatalytic Activity

Their photocatalytic activity was evaluated under UV-visible light to assess the potential of the biosynthesized NCQDs for degrading Rhodamine-B dye. During the experiment, a solution with a fixed concentration of the dye was used, and the procedure was conducted without stirring the sample. The degradation of the dye concentration was monitored at 20-minute intervals using the peak of the pure dye as a benchmark. The results indicate that the dye concentration decreases gradually, though not significantly, over time (Figure 8b).

DOI:https//doi.org/10.22452/mjs.vol43no3.2
Malaysian Journal of Science 43(3): 9-21 (September 2024)

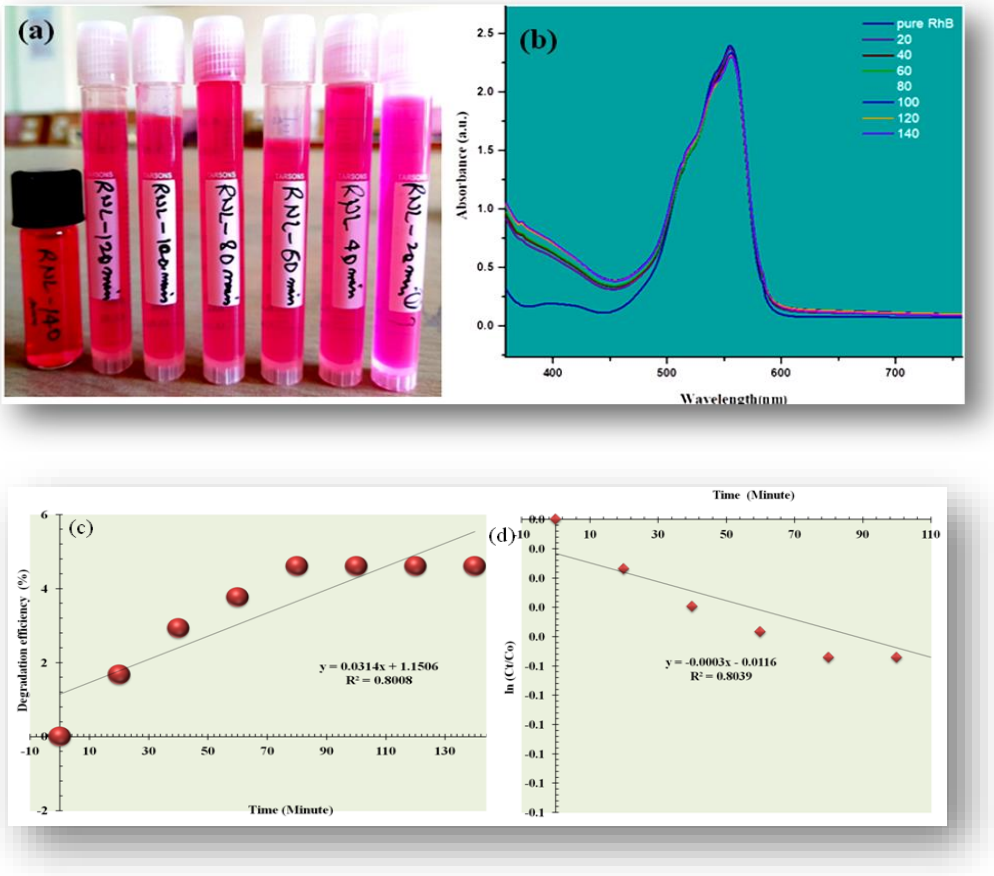

Figure 8. (a) Prepared samples of Rh-B dye **(b)**Plot of absorbance versus wavelength **(c)** Photocatalytic degradation efficiency of dye and **(d)** Kinetic results for the degradation of dye

Figure(8c) illustrates the variation in photocatalytic degradation efficiency over time. The kinetics of the degradation process was analyzed to determine the photocatalytic decolourization's rate constant and correlation coefficient. The correlation coefficient was found to be approximately 0.80, and the reaction rate constant was determined to be 0.003min^{-1} (Figure8d).

5. Conclusion

Rubus niveus was utilized as the carbon source, and ethylenediamine was employed to introduce nitrogen in the hydrothermal method, successfully synthesizing NCQDs. Characterization revealed the fluorescence properties, presence of functional groups, and amorphous structure of the NCQDs. The study demonstrated that this biocompatible material can produce highly fluorescent particles. Additionally, the fluorescence intensity varied with pH, confirming the potential of NCQDs as pH sensors. The correlation coefficient for Rhodamine dye degradation was determinedtobe0.80, indicating its suitability for photocatalytic applications, with potential for further enhancement through additional treatment.

6. Funding

The present work was carried out with the support of seed money (Ref: UU/DRI/SM/2022/13) provided by Uttaranchal University, Dehradun.

7. Acknowledgement

Dr. B.S. Rawat, one of the contributors, expresses gratitude to the Division of research & Innovation, Uttaranchal University, Dehradun for facilitating the research facilities.

8. Conflicts of Interest

The author(s) declare(s) that there is no conflict of interest regarding the publication of this paper

DOI:https//doi.org/10.22452/mjs.vol43no3.2
Malaysian Journal of Science 43(3): 9-21 (September 2024)

5. References

AryaS., MahajanP., MahajanS., KhoslaA., DattR., GuptaV., YoungS.-J., OrugantiS.K.(2021). Review-Influence of Processing Parameters to Control Morphology and Optical Properties of Sol-Gel Synthesized ZnO Nanoparticles. ECS J. Solid State Sci. Technol.10:23002. doi:10.1149/ 2162-8777/abe095

BaiZ. H., ChenR., SiP., HuangY. J., SunH. D., KimD. H. (2013). Fluorescent pH Sensor Based on Ag@SiO_2 Core-Shell Nanoparticle, ACS Applied Materials & Interfaces, 5(12): 5856-5860.

Barati A., Shamsipur M., Abdollahi H. (2016). Metal-ion-mediated fluorescent carbon dots for indirect detection of sulfide ions, Sens. Actuator B: Chem. 230: 289–297.

Basavaiah K., Tadesse A., Ramadevi D., Hagos M., Battu G.(2018).Facile green synthesis of fluorescent carbon quantum dots from citrus lemon juice for live cell imaging, Asian, J. Nanosci. Mater 1:36–46.

Blassan G., Thangaraj P., Sajeesh T., Saravanan S. (2014). Antitumor and wound healing properties of *Rubus niveus* Thunb root. J Environ Pathol Toxicol Oncol.33 (2): 145-158.

Bourlinos A.B., Karakassides M.A., Kouloumpis A., Gournis D., Bakandritsos A., Papagiannouli I. , Aloukos P., Couri S., Hola K., Zboril R., Krysmann M., Giannelis E.P. (2013). Synthesis, characterization and non-linear optical response of organophilic carbon dots, Carbon 61: 640–646.

Carolan D., Rocks C., Padmanaban D.B., Maguire P., Svrcek V., Mariott D.(22017). Environmentally friendly nitrogen-doped carbon quantum dots for next generation solar cells Sustain. Energy Fuels 1:1611–1619.

Chan Y.H., Wu C.F., Ye F.M., Jin Y.H., Smith P.B., Chiu D.T. (2011). Development of Ultrabright Semiconducting Polymer Dots for Ratiometric pH Sensing, Anal. Chem. 83(4): 1448–1455.

Chang K., Zhu Q., Qi L., Guo M., Gao W., Gao Q. (2022). Synthesis and Properties of Nitrogen-Doped Carbon Quantum Dots Using Lactic Acid as Carbon Source. *Materials*. 15(2), 466. https://doi.org/10.3390/ma15020466

Cui L., Ren X., Sun M., Liu H., Xia L. (2021).Carbon Dots: Synthesis, Properties and Applications,Nanomaterials (Basel)11: 3419.

Das B., Dadhich P., Pal P., Srivas P.K., Bankoti K., Dhara S.J. (2014).Carbon nanodots from date molasses: new nanolights for the *in vitro* scavenging of reactive oxygen species, Mater. Chem. B, 2: 6839–6847.

Dash U.N., Dash M.C. (1999). The effect of solvent polarity on the absorption and fluorescence of rhodamine dyes: a linear salvation energy relationship analysis. Journal of Luminescence 82(3): 169-180

DennisA.M., RheeW.J., SottoD., DublinS.N., BaoG. (2012).Quantum Dot–Fluorescent Protein FRET Probes for Sensing Intracellular pH, ACS Nano 6(4):2917–2924.

Dsouza, S. D. (20221). The importance of surface states in N-doped carbon quantum dots. Carbon, 183: 1–11. doi.org/10.1016/j.carbon.2021.06.088 0008

Du F., Zeng F., Ming Y., Wu S. (2013). Carbon dots-based fluorescent probes for sensitive and selective detection of iodide, Microchim. Acta 180:453-460.

Ge G. , Li L., Chen M., Wu X., Yang Y., Wang D., Zuo S., Zeng Z., Xiong W., Guo C. (2022). Green Synthesis of Nitrogen-Doped Carbon Dots from Fresh Tea Leaves for Selective Fe^{3+} Ions Detection and Cellular Imaging, Nanomaterials (Basel):12: 986.

HanJ.Y., BurgessK. (2010). Fluorescent Indicators for Intracellular pH, Chem. Rev. 110: 2709–2728.

Hoan B.T., Tam P.D., Pham V.H. (2019). Green Synthesis of Highly Luminescent Carbon Quantum Dots from Lemon Juice, J. Nanotechnol2019: 1–9.

Jallel J. A., Pramod K. (201). Artful and multifaceted applications of carbon dot in biomedicine, J. Control. Release 269: 302–321.

JinT., SasakiA., KinjoM., MiyazakiJ. (2010). A quantum dot-based ratiometric pH sensor, Chem. Commun. 46: 2408–2410.

KhairolN.F., SapaweN. (2018). Electrosynthesis of ZnO nanoparticles deposited onto egg shell for degradation of Congo red. Mater. Today Proc. 5: 21936–21939.

Khazan, A., Mohammadi A.H., Alimohammadi Z. (2017). Effects of solvent polarity on the absorption and fluorescence spectra of β-carotene in various solvents: A solvatochromic study. Journal of Luminescence 191: 89-95.

Kou, X., Jiang, S., Park, S. J., Meng, L. Y. (2020). A review: Recent advances in preparations and applications of heteroatom-doped carbon quantum dots. Dalton Trans. 49: 6915–6938.

KrysmannM.J., KelarakisA., DallasP., GiannelisE.P. (2012). Formation mechanism of carbogenic nanoparticles with dual photoluminescence emission, J. Am. Chem. Soc. 134:747–750.

LiY., ZhaoY., ChengH.H., HuH.H., ShiG.Q., DaiL.M., QuL.T.(2012). Nitrogen-doped graphene quantum dots with oxygen-rich functional groups, J. Am. Chem. Soc. 134:15–18.

DOI:https//doi.org/10.22452/mjs.vol43no3.2
Malaysian Journal of Science 43(3): 9-21 (September 2024)

Lin Z., Xue W., Chen H., Lin J.M. (22012). Classical oxidant induced chemiluminescence of fluorescent carbon dots, Chem. Commun. 48 (7). 1051e1053. doi: 10.1039/c1cc15290d

Liu C., Zhang P., Tian F., Li W., Li F., Liu W. (2011). One-step synthesis of surface passivated carbon nanodots by microwave assisted pyrolysis for enhanced multicolor photoluminescence and bioimaging, J. Mater. Chem. 21: 13163-13167.

Mosconi D., Mazzier D., Silvestrini S., Privitera A., Marega C., Franco L., Moretto A.(2015). Synthesis and photochemical applications of processable polymers enclosing photoluminescent carbon quantum dots, ACS Nano 9: 4156-4164.

Muhammad F.F., Sulaiman K. (2011). Utilizing a simple and reliable method to investigate the optical functions of small molecular organic flms-Alq3 and Gaq3 as examples. Measurement 44:1468–1474.

Mullen W., McGinn J., Lean M.J., MacLean M.R., Gardiner P., Duthie G.G.(2002). Ellagitannins, flavanoids, and other phenolics in red raspberries and their contribution to antioxidant capacity and vasorelaxation properties. J Agri Food Chem. 50:5191–6.

NieH., LiM.J., LiQ.S., Liang S.J., TanY.Y., ShengL. (2014).Carbon Dots with Continuously Tunable Full-Color Emission and Their Application in Ratiometric pH Sensing, Chem. Mater. 26(10): 3104–3112. doi.org/10.1021/cm5003669

Pancholi B., RanaA.C. (2020). Traditional Uses, Phytochemistry and Pharmacological Aspects of *Rubus niveus* thumb Plant – A Review The J.ournal of Phytopharmacology 9(6): 438-444.

Pires N.R., SantosC.M.W., SousaR.R., de PaulaR.C.M., CunhaP.L.R., FeitosaJ.P.A. (2015). Novel and fast microwave-assisted synthesis of carbon quantum dots from raw cashew gum, J. Braz. Chem. Soc. 26:1274-1282.

QuL.T., Liu V, BaekJ.B., DaiL.M. (2010). Nitrogen-doped graphene as efficient metal-free electrocatalyst for oxygen reduction in fuel cells, ACS Nano. 4:1321–1326.

Raja S., Ramesh V., Thivaharan V. (2015). Green biosynthesis of silver nanoparticles using calliandra haematocephala leaf extract, their antibacterial activity and hydrogen peroxide sensing capability, Arabian J. Chem. DOI: 10.1016/j.arabjc.2015.06.023.

Rooj B., Dutta A., Islam S., Mandal U. (2018). Green Synthesized Carbon Quantum Dots from Polianthes tuberose L. Petals for Copper (II) and Iron (II) Detection, J. Fluoresc 28: 1261–1267.

Salinas-Castillo A., Ariza-Avidad M., Pritz C., Camprubí-Robles M., Fern andez B., Ruedas-Rama M.J., Megia-Fernandez A., Lapresta-Fern andez A., Santoyo-Gonzalez F., Schrott-Fischer A., Capitan-Vallvey L.F. (2013). Carbon dots for copper detection with down and upconversion fluorescent properties as excitation sources, Chem. Commun. 49: 1103-1105.

Sathishkumar G., Gobinath C., Karpaga K., Hemamalini V., Premkumar K., Sivaramakrishnan S. (2012). Phyto-synthesis of silver nanoscale particles using Morinda citrifolia L. and its inhibitory activity against human pathogens, Colloids Surf., B. 95:235-240.

Shamsipur M., Rajabi H. (2014). Pure zinc sulfide quantum dot as highly selective luminescent probe for determination of hazardous cyanide ion, Mater. Sci. Eng. C 36: 139–145.

SinghR., Dutta S. (2018). Synthesis and characterization of solar photoactive TiO2 nanoparticles with enhanced structural and optical properties, Adv. Powder Technol. 29: 211–219.

Su B.N., Pawlus A.D., Jung H.A., Keller W.J., McLaughlin J.L., Kinghorn A. D. (2005). Chemical Constituents of the Fruits of Morinda citrifolia (Noni) and their antioxidant Activity, J. Nat. Prod. 68:592-595.

TantamaM., HungY.P., YellenG.J.(2011).Imaging Intracellular pH in Live Cells with a Genetically Encoded Red Fluorescent Protein Sensor, Am. Chem. Soc. 133: 10034-10037.

Tauc J., Grigorovici R., Vancu A. (1966). Optical properties and electronic structure of amorphous germanium. Physica status solidi (b), 15:627-637.

Wang H., Sun P., Cong S., Wu J., Gao L., Wang Y., Dai X., Yi Q., Zou G. (2016).Nitrogen-Doped Carbon Dots for “green” Quantum Dot Solar Cells, Nanoscale Res. Lett., 11: 1–6.

Wang X., Qu Q., Xu B., Ren J., Qu X. (2011). Microwave assisted one-step green synthesis of cell-permeable multicolor photoluminescent carbon dots without surface passivation reagents, J. Mater. Chem. 21: 2445-2450.

XiaoL., SunH. (2018). Novel properties and applications of carbon nanodots, Nanoscale Horizons, 3(6): 565–597.

Yakuphanoglu F., Erten H. (2005). Refractive index dispersion and analysis of the optical constants’ of an ionomer thin flm. Opt Appl 35(4):969.

ZhangJ., YuS.-H. (2016). Carbon dots: large-scale synthesis, sensing and bioimaging, Mater. Today 19(7):382–393.

ZyoudA.H., ZubiA., ZyoudS.H., HilalM.H., ZyoudS., QamhiehN., HajamohideenA., HilalH.S.(2019). Kaolin-supported ZnO nanoparticle catalysts in self-sensitized tetracycline photodegradation: Zero-point charge and pH effects. Appl. Clay Sci. 182, 105294. doi:10.1016/j.clay.2019.105294

DOI:https//doi.org/10.22452/mjs.vol43no3.2
Malaysian Journal of Science 43(3): 9-21 (September 2024)